Journal of Inorganic Biochemistry 153 (2015) 339–345

Contents lists available at ScienceDirect

Journal of Inorganic Biochemistry

journal homepage: www.elsevier.com/locate/jinorgbio

Gold(III) complexes with hydroxyquinoline, aminoquinoline and quinoline ligands: Synthesis, cytotoxicity, DNA and protein binding studies☆

Cecilia Martín-Santos [a], Elena Michelucci [b], Tiziano Marzo [c], Luigi Messori [c], Piotr Szumlas [d], Patrick J. Bednarski [d], Rubén Mas-Ballesté [a], Carmen Navarro-Ranninger [a], Silvia Cabrera [a,*], José Alemán [e,*]

[a] Departamento de Química Inorgánica (Módulo 7), Facultad de Ciencias, Universidad Autónoma de Madrid, Calle Francisco Tomás y Valiente 7, 28049 Madrid, Spain
[b] Mass Spectrometry Center (CISM), University of Florence, via U. Schiff 6, 50019 Sesto Fiorentino, Florence, Italy
[c] Laboratory of Metals in Medicine (MET MED), Department of Chemistry 'Ugo Schiff', University of Florence, via della Lastruccia 3, 50019 Sesto Fiorentino, Florence, Italy
[d] Pharmazeutische/Medizinische Chemie, Institut für Pharmazie, Ernst-Moritz-Arndt Universität Greifswald, 17487 Greifswald, Germany
[e] Departamento de Química Orgánica (Módulo 1), Facultad de Ciencias, Universidad Autónoma de Madrid, Calle Francisco Tomás y Valiente 7, 28049 Madrid, Spain

ARTICLE INFO

Article history:
Received 1 June 2015
Received in revised form 10 September 2015
Accepted 30 September 2015
Available online 3 October 2015

Keywords:
Gold(III) complexes
Quinoline derivatives
Cytochrome c interaction

ABSTRACT

In this article, we report on the synthesis and the chemical and biological characterization of novel gold(III) complexes based on hydroxyl- or amino-quinoline ligands that are evaluated as prospective anticancer agents. To gain further insight into their reactivity and possible mode of action, their interactions with model proteins and standard nucleic acid molecules were investigated.

© 2015 Elsevier Inc. All rights reserved.

1. Introduction

The therapeutic application of metallic complexes in cancer treatment is one of the main areas of medicinal inorganic chemistry, where cisplatin represents the principal drug in widespread clinical use. In recent years, gold(I) and gold(III) complexes have attracted much attention among medicinal inorganic chemists because of their strong cytotoxicity in vitro and of their different mode of action in comparison to cisplatin [1–12]. Indeed, although platinum(II) and gold(III) complexes are isoelectronic (d^8 configuration) and isostructural (square planar geometry), they were found to show different biological profiles and mechanisms of action [13]. For platinum(II) complexes, DNA is commonly believed to be the primary target while inhibition of a few crucial proteins seems to be the main mechanism of action for cytotoxic gold complexes. In addition, ligand exchange is faster in gold(III) complexes compared to platinum(II) ones. In this sense, the chelation of the metallic centre with multidentate ligands have shown to enhance the stability of the complex, but an excessive stabilization of the gold centre may be detrimental to the biological activity (e.g. Au(cyclam)) [14]. The selection of ligands is also crucial to modulate the oxidizing character of the gold(III) centre and to decrease its pronounced tendency to be reduced to gold(I). In the last few years, new promising antitumor gold(III) complexes containing nitrogen-donor polyaromatic ligands, such as terpyridine and phenanthroline derivatives (see Chart 1) have been reported to control these two features [15,16].

In the context of polyaromatic ligands, hydroxyquinolines were reported to be promising therapeutic agents for Alzheimer's dementia due to strong complexation with copper and zinc ions which are involved in the ß-amyloid peptide aggregation that causes neuronal loss in Alzheimer's disease patients [17–20]. Moreover, hydroxyquinolines are known to exhibit a variety of biological activities [21–25]. In particular, clioquinol (5-chloro-7-iodo-quinolin-8-ol) is currently commercially available as an antifungal and antibacterial drug. Regarding the anticancer activity of the hydroxyquinolines, a number of interesting features were highlighted. They are classified as proteasome inhibitors through complexation with copper ions [26–29]; they induce apoptosis of human cancer cell lines by targeting zinc to lysosomes [30]; they are NF-kappa β inhibitors [31,32], or stimulate macrophages to release tumor necrosis factor alpha [33] among other anticancer activities. All these applications are related to the use of hydroxyquinolines as scavengers of metals involved in the pathogenesis of various diseases. Recently, we have synthesized new platinum complexes [34–36] containing hydroxyquinolines in their structure and could demonstrate high in vitro antitumor activity and their interactions with DNA [37]. Therefore, we considered feasible the synthesis of new gold complexes

Abbreviations: EDTA, Etilendiaminotetraacetic acid; PBS, Phosphate buffered saline; TAE buffer, Tris-acetate–EDTA buffer.

☆ This manuscript is dedicated to Prof. Giovanni Natile.

* Corresponding authors.
E-mail addresses: silvia.cabrera@uam.es (S. Cabrera), jose.aleman@uam.es (J. Alemán).
URL: http://www.uam.es/jose.aleman (J. Alemán).

http://dx.doi.org/10.1016/j.jinorgbio.2015.09.012
0162-0134/© 2015 Elsevier Inc. All rights reserved.

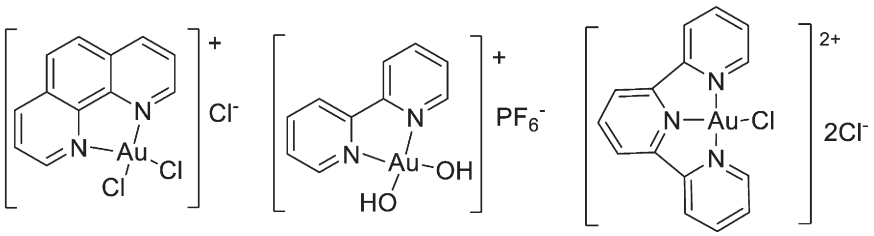

Chart 1. Antitumor active gold complexes containing nitrogen-donor polyaromatic ligands.

analogous to the platinum ones and their possible antiproliferative activity.

In the present study, we report on the synthesis and characterization of new gold(III) complexes containing hydroxyquinolines as ligands (Chart 2, complexes **2**). To explore potential structure-activity relationships, the role of the coordinating atom (oxygen) of the quinoline ligand was investigated by the preparation of one complex with an amino coordinating group (complex **3**). In addition, the synthesis of the quinoline-monocoordinated complex **4** was shown by the chelation effect of the ligand in the cytotoxic activity. The stability and electrochemical properties of the complexes were determined, and the antiproliferative evaluation of the compounds was done in vitro with four human cancer cell lines. Finally, we studied the interactions of these complexes with DNA and with model proteins like cytochrome c to establish adducts formation at the biomolecular level.

2. Experimental

2.1. Material and methods

All reagents and materials were purchased from commercial sources and used without further purification. pBR322 plasmid DNA was purchased from GeneCust-thermo scientific. NMR spectra were acquired on a Bruker 300 spectrometer running at 300, and 75 MHz for ^{1}H, and ^{13}C, respectively. Chemical shifts (δ) are reported in ppm relative to residual solvent signals ($CDCl_3$: 7.26 ppm for ^{1}H NMR, 77.0 ppm for ^{13}C NMR; CD_2Cl_2: 5.32 ppm for ^{1}H NMR, 53.84 for ^{13}C NMR; DMSO-d_6: 2.50 ppm for ^{1}H NMR, 39.52 for ^{13}C NMR). ^{13}C NMR spectra were acquired on a broad band decoupled mode.

2.2. General procedure for the synthesis of complexes *2a–c*, *3* and *4*

To a solution of the corresponding ligand **1** (0.85 mmol) in 5 mL of MeOH was added Na[$AuCl_4$] (0.68 mmol) at rt. The resulting suspension was stirred for 24 h and then the solid product was filtered, washed with cold methanol and cold ether, and dried at 60 °C over 24 h.

2.2.1. [$AuCl_2$(8-O-quinoline)] (*2a*)

Green solid. Yield: 46%. ^{1}H NMR (300 MHz, CD_2Cl_2) δ: 9.14 (dd, J = 5.5, 1.2 Hz, 1H), 8.61 (dd, J = 8.3, 1.2 Hz, 1H), 7.73 (dd, J = 8.4, 5.5 Hz, 1H), 7.65 (t, J = 8.0 Hz, 1H), 7.40 (dd, J = 8.1, 0.7 Hz, 1H), 7.31 (dd, J = 8.0, 0.8 Hz, 1H). ^{13}C NMR (75 MHz, DMSO-d_6) δ: 164.7, 145.2, 143.2, 142.6, 131.9, 131.4, 123.0, 117.5, 114.9. MALDI-MS: 411 ($[M]^+$), 376 ($[M\text{-}Cl]^+$), 341 ($[M\text{-}2Cl]^+$). Anal. Calcd. For $C_9H_6AuCl_2NO$ (%): C, 26.24; H, 1.47; N, 3.40. Found (%): C, 26.26; H, 1.61; N, 3.31.

2.2.2. [$AuCl_2$(5-Cl-8-O-quinoline)] (*2b*)

Green solid. Yield: 76%. ^{1}H NMR (300 MHz, $CDCl_3$) δ: 9.25 (dd, J = 5.4, 1.2 Hz, 1H), 8.91 (dd, J = 8.6, 1.2 Hz, 1H), 7.85 (dd, J = 8.6, 5.4 Hz, 1H), 7.72 (d, J = 8.5 Hz, 1H), 7.26 (d, J = 8.5 Hz, 1H). ^{13}C NMR (75 MHz, CD_2Cl_2) δ: 164.7, 145.7, 143.8, 140.9, 131.8, 129.6, 123.2, 120.9, 115.9. ESI + MS (TOF): 444.24 ($[M]^+$). Anal. Calcd. For $C_9H_5AuCl_3NO$ (%): C, 24.21; H, 1.13; N, 3.14. Found (%): C, 24.38; H, 1.29; N, 3.09.

2.2.3. [$AuCl_2$(8-NH_2-quinoline)]Cl (*3*)

Purple solid. Yield: 52%. ^{1}H NMR (300 MHz, $CDCl_3$) δ: 9.37 (dd, J = 5.4, 1.2 Hz, 1H), 8.50 (dd, J = 8.3, 1.2 Hz, 1H), 7.71 (dd, J = 8.3, 5.4 Hz, 1H), 7.51 (t, J = 7.9 Hz, 1H), 7.23 (d, J = 7.6 Hz, 1H), 7.03 (dd, J = 7.8, 0.7 Hz, 1H), 6.50 (brs, 2H). ^{13}C NMR (75 MHz, DMSO-d_6) δ: 155.6, 146.0, 143.0, 139.4, 131.7, 131.0, 123.2, 116.2, 112.8. FAB-HRMS: $[M]^+$ calcd. For $[C_9H_8AuCl_2N_2]^+$: 410.9725, found: 410.9717. Anal. Calcd. For $C_9H_8AuCl_3N_2$ (%): C, 24.16; H, 1.80; N, 6.26. Found (%): C, 24.48; H, 1.84; N, 6.52.

2.2.4. [$AuCl_3$(quinoline)] (*4*)

Yellow solid. Yield: 62%. ^{1}H NMR (300 MHz, $CDCl_3$) δ: 9.10 (dd, J = 5.5, 1.3 Hz, 1H), 8.82 (dd, J = 8.5, 0.8 Hz, 1H), 8.65 (d, J = 8.2, 1H), 8.15–8.06 (m, 2H), 7.91–7.84 (m, 1H), 7.80 (dd, J = 8.2, 5.5 Hz, 1H). ^{13}C NMR (75 MHz, $CDCl_3$) δ: 152.0, 143.7, 143.0, 134.1, 131.3, 129.7, 129.1, 126.4, 123.1. Anal. Calcd. For $C_9H_7AuCl_3N$ (%): C, 24.99; H, 1.63; N, 3.24. Found (%): C, 24.63; H, 1.73; N, 3.12.

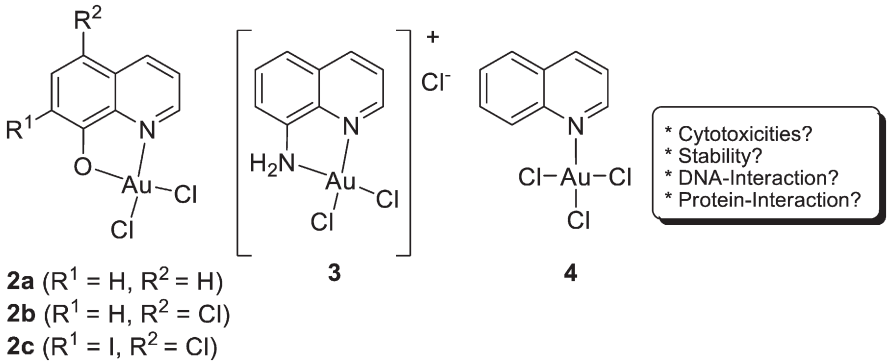

2a (R^1 = H, R^2 = H)
2b (R^1 = H, R^2 = Cl)
2c (R^1 = I, R^2 = Cl)

3 **4**

Chart 2. Gold(III) complexes synthesized and studied in the present work.

2.3. Crystallographic structure determination

Crystals of compound **2a** or **4** were obtained by slow evaporation of a solution of the corresponding compound in $CHCl_3$. These crystals were mounted at low temperature in inert oil on a glass fibre. Data were collected on a Bruker X8 APPEX II CCD-based diffractometer, equipped with a graphite monochromated MoKα radiation source (λ = 0.71073 Å).

The crystal data, data collection, structural solution, and refinement parameters for the complexes are summarized in Table 1. Data were integrated using SAINT [38] and an absorption correction was performed with the program SADABS [39]. The structures were solved by direct methods using SHELXTL [40], and refined by full-matrix least-squares methods based on F^2. All non-hydrogen atoms were refined with anisotropic thermal parameters. All H atoms were computed and refined with an overall isotropic temperature factor using a riding model.

2.4. Stability assays

The stability of the compound **2a** was performed in DMSO and DMF, saline solution (0.9% NaCl) and PBS (0.01 M phosphate buffer, 0.0027 M potassium chloride and 0.137 M sodium chloride, pH 7.4), and determined by UV–Vis spectroscopy. For the stability in organic solvents, a 1 mM solution of complex **2a** in DMSO or DMF was kept at rt., and at different time points the electronic spectra were recorded by using an Agilent 8453 UV–vis spectrophotometer (see Supporting information (S.I.) for graphs). For stabilities in saline or PBS solutions, 10 μL of a stock solution of compound **2a** (10 mM in DMSO) were diluted in saline solution or PBS up to 2.0 mL (final concentration 50 μM). The solution was incubated at 37 °C and the electronic spectra were recorder over 24 h.

2.5. Electrochemistry

The electrochemical experiments were conducted in a 1.0 mM solution of the corresponding complex in CH_2Cl_2 containing $(Bu_4N)(PF_6)$ (0.1 M) at 50 mV/s. The working electrode was a glassy carbon disk (2.8 mm diameter) and the counter electrode was a platinum wire and the reference electrode was Ag/AgCl.

Table 1
Crystal data and structure refinement for complexes **2a** and **4**.

Complex	2a	4
Empirical formula	$C_9H_6AuCl_2NO$	$C_9H_7AuCl_3N$
Mw	412.01	432.47
Temperature (K)	296 (2)	296 (2)
Wavelength (Å)	0.71073	0.71073
Cryst. system	Monoclinic	Monoclinic
Space group	P 2_1/n	P 2_1/c
a (Å)	4.229 (1)	7.5337 (1)
b (Å)	17.357 (6)	8.3674 (2)
c (Å)	13.814 (5)	18.2547 (4)
α (deg)	90	90
β (deg)	96.86 (2)	90.08 (1)
γ (deg)	90	90
Volume (Å^3)	1006.7 (6)	1146.2 (4)
Z	4	4
Density (calcd) (g/cm^3)	2.718	2.506
Abs. coeff (mm^{-1})	15.105	13.492
F(000)	752	792
Crystal size (mm^3)	0.01 × 0.12 × 0.35	0.06 × 0.16 × 0.18
Reflections collected	15,740	38,284
Independent reflections	2035 [R(int) 0.0520]	2094 [R(int) 0.0352]
No. of data/restraints/params.	2035/0/127	2094/0/127
Goodness-of-fit on F^2	1.001	1.003
Final R indices [I > 2σ (I)]	R_1 = 0.0362; wR_2 = 0.0978	R_1 = 0.0141; wR_2 = 0.0339
Largest diff peak hole (eÅ^{-3})	2.016 and −1.268	0.716 and −0.647

2.6. Cancer cell antiproliferation studies

Human tumor cell lines A427 (lung cancer cell line), LCLC-103H (large cell lung cancer), SISO (uterine adenocarcinoma) and 5637 (human bladder carcinoma) were used in this study. All cell lines were obtained from the German Collection of Microorganisms and Cell Culture (DSMZ, Braunschweig, Germany). The antiproliferative effects of the complexes on human cancer cells after a 96 h exposure were determined by using a microtiter assay based on the staining of the cell mass with crystal violet, as reported in detail previously [41]. Briefly, the compounds were dissolved in spectral grade DMF and serially diluted with DMF five times to give concentrations 500-fold the final test concentrations. These stock solutions were diluted 500-fold into RPMI-1640 medium containing 10% fetal calf serum to give the working solutions. To each well of the microtiter plate, which contained cells seed out 24 h before in 100 μL culture medium, were added 100 μL of the working solutions to give final concentrations in culture medium 1000-fold less than the stock solutions. Cells exposed only to 0.1% DMF were run as untreated controls. After 96 h continuous exposure, culture medium was removed from the plates and cells were stained for 20 min with a 0.02% crystal violet solution in water. The dye solution was removed from the plates, which were washed with water for 30 min before a 70% ethanol/water mixture was added (100 μL/well) to dissolve the cell-bound dye. Optical density was measure with a plate reader Anthos 2010 set at λ = 570 nm. MS-Excel was used to estimate the IC_{50} values (concentration leading to a 50% reduction in cell growth) by linear regression analysis of the T/C_{corr} values versus log concentration [41].

2.7. DNA electrophoresis

The DNA interaction was evaluated by monitoring the mobility of supercoiled plasmid DNA covalently closed circular (cc) and open circular DNA (oc), as previously described [42]. The DNA binding studies were done in a total reaction volume of 20 μL using pBR322 plasmid DNA. Each reaction mixture containing 4 μL of DNA-pBR322 (10 ng/mL stock) in 10 mM Tris–HCl (pH = 7.6) and 1 mM EDTA was incubated with the gold compounds at several r_i (input molar ratio of Au/nucleotides) values (0.01 to 0.5) using the corresponding amount of gold complex from either 10, 20 or 50 μM stock solution (the stock solutions were prepared from the corresponding compound solution in DMSO (1 mg/mL) and water until reaching the desired concentration). Samples were typically incubated for 24 h at 37 °C. After incubation, 2 μL of a loading dye containing 50% glycerol, 0.25% bromophenol blue and 0.25% xylene cyanol was added. The total of the sample (20 μL) was loaded in the wells of a 0.8% agarose gel. Electrophoresis was carried out for 2 h at approximately 70 V. The gels were then stained in 250 mL of TAE buffer containing 64 μL from a 10 mg/mL stock solution of ethidium bromide for 30 min. Controls of non-incubated plasmid and of plasmid incubated with DMSO were loaded on each run. Bands were visualized under UV light, and images were captured with an AlphaImagerEP (Alpha Innotech). All samples in each figure were obtained from the same run.

2.8. Interaction with cytochrome C

A solution of compounds **2a**–**b** and **3** (3×10^{-4} mol L^{-1}) with cytochrome c (3:1 complex/protein molar ratio) was incubated in ammonium acetate buffer (pH = 6.8) at 37 °C. After 24 h, the incubation solution was diluted 20-fold with water before ESI MS spectra were recorded by direct introduction at 5 μL min^{-1} flow rate in an Orbitrap high-resolution mass spectrometer (Thermo, San Jose, CA, USA), equipped with a conventional ESI source. The working conditions were the following: spray voltage 3.1 kV, capillary voltage 45 V, capillary temperature 220 °C, tube lens voltage 230 V. The sheath and the auxiliary gases were set, respectively, at 17 (arbitrary units) and 1 (arbitrary

units). For acquisition, Xcalibur 2.0. software (Thermo) was used and monoisotopic and average deconvoluted masses were obtained by using the integrated Xtract tool. For spectrum acquisition a nominal resolution (at m/z 400) of 100,000 was used.

3. Results and discussion

3.1. Synthesis and structural characterization

The optimal reaction conditions for the synthesis of the gold(III) complex **2a** were explored (see Table S1 in S.I.). Initial attempts were carried out starting from a solution of sodium tetrachloroaurate(III) and 1.0 equivalent of ligand **1a** in MeOH. In these conditions, complex **2a** was formed but in moderate yield (38%). We have found in our previous work [37] that the addition of NaOH enhanced the nucleophilicity of the hydroxyquinoline and improved the complexation to the metal (platinum in that case). However, the use of 1.0 equivalent of NaOH led to the reduction of the gold(III) salt (entry 2). In attempts to improve the yield, we screened other solvents, such as water or mixtures of MeOH/acetone, and other reaction conditions but without success. A slight decrease in the equivalents of the ligand **1a** (0.8 equiv.) did not increase the yield of complex **1a** (39%); whereas the addition of 1.2 equivalents of ligand allowed the isolation of the complex **1a** in better yield (46%). Thus, these reaction conditions (1.2 equivalents of ligand in MeOH as solvent) were selected for the synthesis of the other complexes.

Copper and platinum complexes with halogen-substituted hydroxyquinolines have been also reported to have good cytotoxic activity [37,43]. For this reason, we synthesized the gold complex **2b** with a chlorine at 5-position (R^2) of the hydroxyquinoline in 76% yield (Chart 2). By contrast, the complexation of the clioquinol (5-chloro-7-iodo-8-hydroxyquinoline, ligand **1c**) with an iodine atom at *ortho*-position of the hydroxyl group to the Au(III) was not possible. The addition of NaOAc or K_2CO_3 as base was also studied and only starting material was detected in the crude NMR.

With the aim of obtaining a preliminary structure-activity relationship, two additional complexes were synthesized (complexes **3** and **4**, Chart 2). In the case of complex **3**, the hydroxyl group of the quinoline was substituted by an amino group to obtain the corresponding cationic gold(III) complex in 52% yield. In addition, the non-chelated complex **4** was also prepared starting from quinoline (62% yield) to investigate the biological effect of chelation of the ligand to the metal.

In order to verify the complexation of the corresponding ligand **1** to the gold centre, the ^1H and ^{13}C NMR chemical shifts of the complexes were compared to those of the free ligand. In all the complexes, the highest deshielding was found for H-1 (the proton adjacent to the pyridyl nitrogen) in the ^1H NMR spectra. For example, in complex **3** a downfield shift of 0.6 ppm is observed for the H-1 signal, due to the deshielding produced by the electron-withdrawing gold centre.

To determine the structure of these gold(III) complexes, suitable crystals of compound **2a** were analysed by X-ray diffraction (Fig. 1) (CCDC 986616 contains the supplementary crystallographic data, see S.I. for more details). The molecule is formed through coordination of the deprotonated 8-hydroxyquinoline to the gold centre and of two chloride ligand atoms. This complex (**2a**) presents a distorted square planar geometry (see S.I. for more details), due to the restrictions imposed by the five-membered ring formation of the chelating ligand (Table 2). The angle N(1)-Au(1)-O(1) and N(1)-Au(1)-Cl(1) are quite far from 90° (82.7° and 96.8°, respectively). In addition, crystals of complex **4** were obtained from a chloroform solution and analyzed by X-ray diffraction (Fig. 2) (CCDC 1045573 contains the supplementary crystallographic data, see S.I. for more details). In these crystals, the Au(III) adopts a square planar geometry (see S.I. for more details), being the angles N(1)-Au(1)-Cl(2) and N(1)-Au(1)-Cl(4) close to 90° (88.8° and 89.0°, respectively, Table 3). In addition, the three Au-Cl distances are very similar to each other (see Table 3), and no significant differences were found with the related distances in complex **2a**.

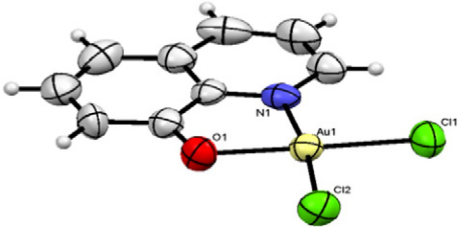

Fig. 1. ORTEP view of complex **2a**.

Structure of complexes **2b** and **3** have not been solved by X-ray crystallography. However, although not unequivocally, the structure assigned is the homologous to the observed for **2a**. Such assignment was based on the spectroscopic and spectrometric data, which consistently fits with the present proposal.

3.2. Stability studies

Before the biological studies, it is important to assess the stability in solution of these gold complexes. Most of these studies are concerned to their stability in aqueous solution. However, the stability of the complexes in the organic solvent used to prepare the stock solution for the biological assays is crucial as demonstrated by Patra et al. [44]. They have reported that DMSO stock solutions of Ru complexes evolve very fast ligand dissociation and coordination of the DMSO, and more importantly, the equilibrium between the complexes with coordinated and uncoordinated DMSO influences the biological activity. The influence of DMSO in the biological activity of metallodrugs has been also reported by Hall et al. [45]. They demonstrated that DMSO — used for the formulation of the compounds — inhibits the cytotoxicity of platinum drugs such as cisplatin and carboplatin due to the coordination of the DMSO to the complexes. For all these reasons, we carried out stability assays of complex **2a** in DMSO and DMF, which are the solvents used for preparing the stock solutions for the interaction studies and biological assay, respectively. The incubation of 1 mM solution of complex **2a** in DMSO at rt. was monitored by UV–Vis spectroscopy for a period of 24 h. The spectrum of the DMSO solution of complex **2a** was unaltered along the time, showing the stability of **2a** in DMSO. However, a slightly decrease in the intensity of the bands after 24 h was observed in the UV–Vis spectrum of the DMF solution of **2a** (see graphs in S.I.). We think that a Cl-DMF exchange reaction is taking place during the incubation of the gold(III) complexes, although the kinetics of this reaction is slower than that observed for the Ru complexes. In addition, DMSO or DMF solutions of complex **2a** can be stored at −20 °C for up to 10 days.

Next, we also studied the stability of complex **2a** in saline solution (0.9% NaCl), and in the reference physiological buffer solution (PBS)

Table 2
Selected bond lengths [Å] and angles [°] for complex **2a**.

Bond lengths (Å)	
Au(1)-N(1)	2.017 (9)
Au(1)-O(1)	2.016 (7)
Au(1)-Cl(1)	2.276 (3)
Au(1)-Cl(2)	2.264 (3)
C(8)-O(1)	1.363 (13)
C(9)-N(1)	1.365 (13)
Angles (°)	
N(1)-Au(1)-O(1)	82.7 (3)
N(1)-Au(1)-Cl(2)	172.3 (3)
O(1)-Au(1)-Cl(2)	89.7 (2)
N(1)-Au(1)-Cl(1)	96.8. (3)
O(1)-Au(1)-Cl(1)	178.9 (2)
Cl(2)-Au(1)-Cl(1)	90.8 (1)

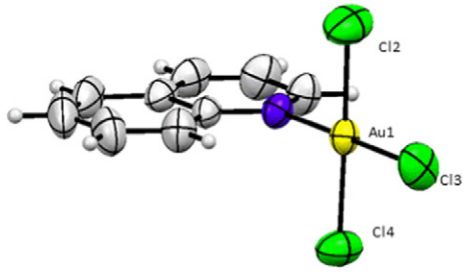

Fig. 2. ORTEP view of complex **4**.

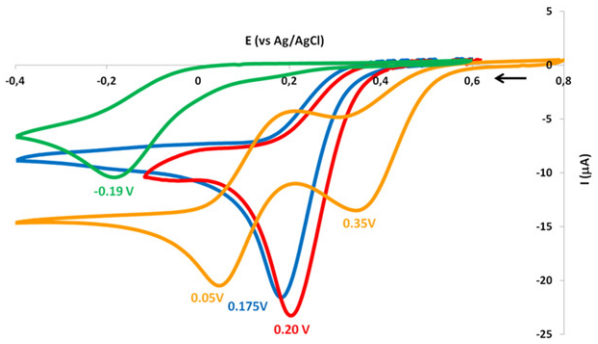

Fig. 3. Cyclic voltammograms of 1.0 mM (0.1 M (Bu_4N)(PF_6)) solution of complexes **2a** (blue) and **2b** (red), **3** (green) and **4** (orange) in CH_2Cl_2 at 50 mV/s.

(see graphs in S.I.). In both solutions, the stability of complex **2a** was poor after 24 h, showing a decrease in the intensity of the bands and a bathochromic shift of the LMCT transition band in the spectrum. We suggest that hydrolysis of the complex is probably taking place both in saline and in buffer solutions by replacement of the chloride ligand by water molecule. Although these complexes are not stable in aqueous solutions, the complexes are very cytotoxic as will be described below, and more deeply studies to identify the intermediate species that are responsible for the biological activity will be carried out.

3.3. Electrochemistry

The redox properties of the complexes were studied by cyclic voltammetry to determine their reduction potentials. These studies were conducted using 1.0 mM solution of the corresponding complex in CH_2Cl_2 to avoid the formation of species by the coordination of the solvent to the gold center. The cyclic voltammetric curves of complexes **2a**, and **2b** showed only one reduction process which was irreversible even at scan rates higher than 200 mV/s (Fig. 3). This reduction process was determined to be two electron/molecule by chronoamperometry and, thus, the reduction of the gold(III) complexes proceeds through an Au(III)/Au(I) step. The intensity and the reduction potential values of complexes **2a** and **2b** were very similar, suggesting a scarce influence in the electronic density of the gold(III) metal of the chloro atom at 5-position. However, by changing the oxygen coordinated atom of the quinoline ligand, by the amino group, a significant change in the reduction potential has been observed.

Curiously, while compound **3** is cationic, its reduction is thermodynamically less favored than those of compounds **2a** and **2b**, which are neutral species. Consideration of the overall charge of compounds would lead to expect the opposite trend. However, in this case the main factor to be considered is the balance between the different Au^{3+}-O/Au^{+}-O and Au^{3+}-N/Au^{+}-N Metal-Ligand interactions. The trend experimentally observed indicates that the donating ability of amino group stabilizes the Au(III) oxidized species more efficiently than the hydroxy group. The lower intensity of the electrochemical signal found for compound **3** can be due to its poor solubility as observed by its incomplete dissolution while attempting to prepare 1 mM solutions.

Table 3
Selected bond lengths [Å] and angles [°] for complex **4**.

Bond lengths (Å)	
Au(1)-N(1)	2.032 (1)
Au(1)-Cl(2)	2.276 (1)
Au(1)-Cl(3)	2.257 (1)
Au(1)-Cl(4)	2.261 (1)
C(1)-N(1)	1.313 (4)
Angles (°)	
N(1)-Au(1)-Cl(2)	88.8 (3)
N(1)-Au(1)-Cl(3)	179.3 (8)
N(1)-Au(1)-Cl(4)	89.0 (3)
Cl(3)-Au(1)-Cl(2)	91.0 (3)

A different scenario was found for complex **4**. As shown in Fig. 3 complex **4** shows two consecutive reductions: an irreversible one at a more positive potential than complexes **2a** and **2b** and a second reversible process at a more negative potential than those observed for **2a** and **2b**. Under the same conditions than for compounds **2a** and **2b**, the electrochemical signal of **4** have approximately half of the intensity. Thus, apparently **4** undergoes two different monoelectronic processes. Quinoline ligand is electroactive at potentials close to −2 V *vs* Ag/AgCl which falls far away from the processes observed herein. Consequently, although coordination to Au(III) centres is expected to shift reduction potential towards more positive values, and given the proximity of reduction potentials of **4** to those of the other compounds studied herein, it seems reasonable to assign electroactivity to metal centre reductions. Probably, first a reduction that formally involves one electron per molecule is coupled to chemical evolution that implies dimerization to form a putative Au(III)-Au(I) species, which can be reversibly reduced to a Au(I)-Au(I) product. Despite the electrochemical pathways are not unequivocally determined, electrochemistry measurements offer a definite evaluation of redox stability of the compounds obtained. Therefore, the most stable complex versus reductive evolution is **3**, followed by **2a** and **2b**, which show very similar behavior. Finally, **4** is the more easily reduced complex of the studied series. Such enhanced susceptibility towards reduction probably makes **4** unstable on biological media, which can be one of the causes of its poor cytotoxic activity, as shown below.

3.4. Antiproliferative activity

The antiproliferative activity of these gold(III) complexes was subsequently evaluated against a panel of representative human tumor cell lines including A427 (lung cancer cell line), LCLC-103H (large cell lung cancer), SISO (uterine adenocarcinoma) and 5637 (human bladder carcinoma) by using the crystal violet staining assay [41]. In each human tumor cell line compounds **2a** and **2b**, which only differ in the substitution at 5-position (H or Cl), the cationic complex **3** which contains an amino chelating group instead of oxygen and the mono-coordinated complex **4** were investigated. The experimental IC_{50} values are summarized in Table 4 and compared to those of cisplatin after 96 h of treatment.

Remarkably, **2a**–**b** and **3** showed stronger antiproliferative potency than cisplatin in almost all cases (Table 4), which was most evident in the case of the A427 lung cancer cell line; in fact, **2b** was 10 times more potent than cisplatin in this cell line. The obtained results showed that the substitution of an oxygen by nitrogen atom had only a minimal effect on the antiproliferative activity (compared **2a** and **3**, Table 4). Thus, both neutral and cationic quinoline Au(III)-complexes would appear to enter cells and slow their growth. In the case of the A427 and 5637 lines, the substitution of a chlorine atom into the quinoline ring

Table 4
Antiproliferative IC_{50} (μM) values after a 96 h treatment of four human cancer cell lines (averages and standard deviations of at least 3 independent determinations except where noted).

Complex	IC_{50} (μM) ± SD			
	A427	LCLC-103H	SISO	5637
2a	0.37 ± 0.17	0.26 ± 0.16	0.31 ± 0.08	0.23 ± 0.22
2b	0.19 ± 0.09	0.22[a]	0.40 ± 0.28	0.06 ± 0.02
3	0.23[a]	0.29[a]	0.73 ± 0.43	0.26 ± 0.22
4	nd	>10	>10	>10
Cisplatin[b]	1.96 ± 1.54	0.90 ± 0.19	0.24 ± 0.06	0.35 ± 0.10

nd: not determined.
[a] N = 2.
[b] Values from Ref [41].

brought about a noticeable increase in antiproliferative activity (compare **2b** with **2a**). The non-chelating complex **4** was much less potent than the three compounds with chelate rings, with IC_{50} values above 10 μM in the three cell lines investigated.

3.5. Interactions with DNA

Most biologically active gold compounds display only weak interactions with DNA in contrast to the strong coordinative interactions of platinum complexes with DNA nucleobases. The effect of our gold complexes on the DNA tertiary structure was evaluated by their ability to alter the electrophoretic mobility of the covalently closed circular (cc) and open circular (oc) forms of pBR322 plasmid DNA. In this type of experiment, the covalent binding of cisplatin to pBR322 plasmid DNA produces a decrease in the mobility of the cc form and an increase in the mobility of the oc form. In Fig. 4 the electrophoretic mobility of pBR322 DNA incubated with different concentrations of the Au complex **2a** (r_i) and also with different concentrations of the ligand 8-hydroxyquinoline is shown. We noticed that the reactivity pattern of complex **2a** was very different to cisplatin. In fact, the gold(III) complex did not affect the mobility of the oc form while the cc form disappears at r_i higher than 0.12 and no coalescent point was detected. As expected, 8-hydroxyquinoline ligand did not change the mobility of any of the forms of the plasmid DNA (Fig. 4b). These results suggest that only a weak interaction between **2a** and plasmid DNA may take place and that DNA accordingly may not be the main target. For this reason, interactions with protein targets were studied.

3.6. Reactions with cytochrome C

To gain deeper insight into the specific reactivity of these Au(III) complexes with other potential biomolecular targets, **2a**–**b** and **3** were allowed to react with cytochrome c (cyt c), which is often used as a model protein for metalation studies [46]. The cyt c protein was reacted with an excess of the corresponding Au(III) complex (see S.I.). Notably, the resulting ESI-MS spectra recorded after 24 h showed that incubation of cyt c with these gold(III) complexes leads to the formation of metal-protein adducts in appreciable amounts (Fig. 5). This is clearly documented by the appearance of peaks of higher molecular mass than those assigned to the native protein falling at 12,358.3 Da. The most reactive complex toward cyt c is **2a**. Both **2a** and **2b** reacted with the protein just through coordination of the naked Au^+ cation with loss of the ligand (see simulations in S.I.). Multimetalated adducts have been detected for all complexes (see peaks Au^+ (12,554.3 Da), 2 Au^+ (12,750.2 Da), 3 Au^+ (12,946.2) or 4 Au^+ (13,143.1)). Interestingly, at variance with complexes 2a (in bold) and 2b (in bold), for complex **3** it was possible to detect binding to cyt c with ligand retention. From the simulation compared with the experimental spectra, we can assess that in this case the binding seems to be occuring through simultaneus coordination of both Au^{3+} and Au^+ ions (see S.I.). The latter features could be interpreted as a process that first implies the Au^{3+} coordina-

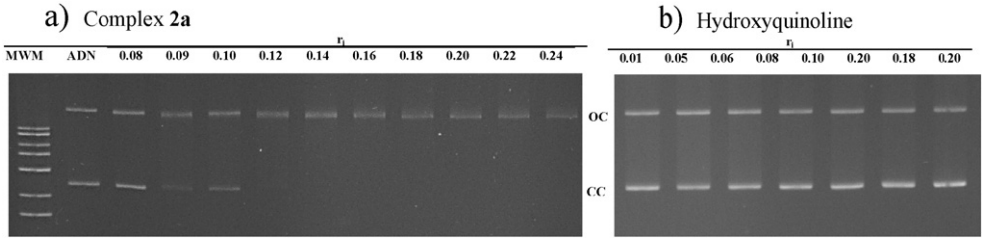

Fig. 4. Interaction of pBR322 plasmid DNA with increasing amounts of complex **2a** (a) and 8-hydroxyquinoline (b) after 24 h of incubation at 37 °C. Forms cc and oc are closed circular and open circular forms of DNA, respectively. r_i: the molar ratio of added gold complex (or compound) per nucleotide.

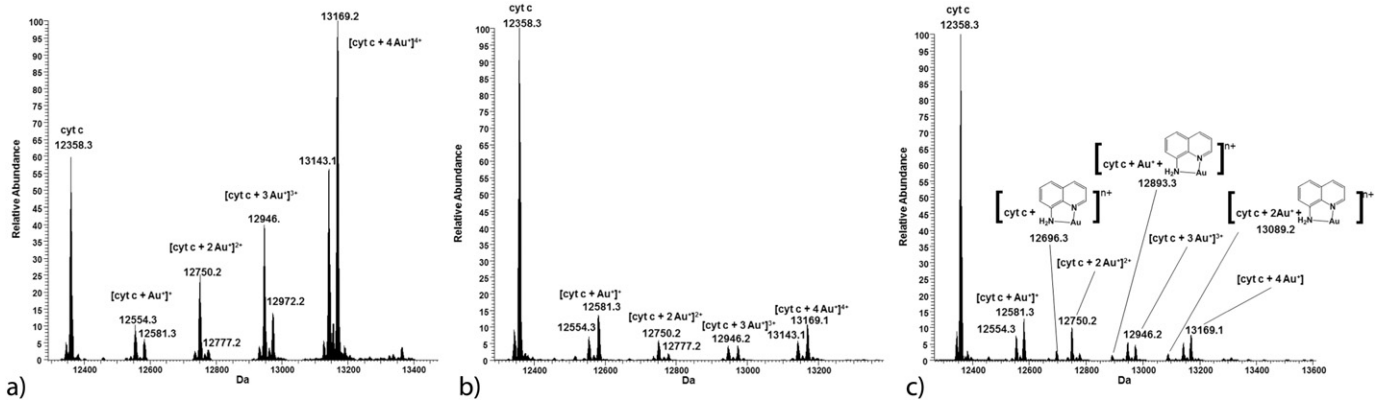

Fig. 5. LTQ-Orbitrap ESI-MS spectra of cyt c (12,358.3 Da) treated with gold compounds (a) **2a**, (b) **2b** and **3** (c) after 24 h of incubation. Cyt c adducts are formed with Au^+ (12,554.3 Da), 2 Au^+ (12,750.2 Da), 3 Au^+ (12,946.2) or 4 Au^+ (13,143.1) bound to the protein. The peaks of Cyt c with a complex **3** (12,696.3 Da), **3** + Au (12,893.3) and **3** + 2Au (13,089.2) are also visible.

tion (with ligand conservation) followed by Au^{3+} reduction to Au^{+} with loss of ligand.

4. Conclusions

We have found that clioquinol and its analogues, which have been used in medicinal chemistry as metal-protein attenuating compounds, are excellent ligands for the synthesis of new gold(III) complexes, some of which show favorable antiproliferative activities. The antiproliferative activity assays conducted with four distinct human solid tumor cell lines show that three out of four tested gold(III) complexes are more active than cisplatin. In particular, the 8-hydroxyquinoline ligand affords the complex with the highest antiproliferative activity in all studied cell lines. DNA interaction assays with the supercoiled pBR322 plasmid DNA have demonstrated that the interactions of these gold(III) complexes with DNA are generally weak. On the other hand, a remarkable reactivity was detected between the study compounds and the model protein cyt c with formation of various kinds of adducts. These results suggest that the cellular effects produced by these gold compounds may be predominantly mediated by interaction with relevant protein targets. For this reason, a more extended investigation will be carried out with the aim of identifying plausible targets related to the cytotoxic effect of these complexes.

Author contributions

C. M. carried out the synthesis, stability and characterization studies. L. M., E. M. and T. M. carried out the mass spectrometry experiments. P. B. and P. S. have evaluated the biological activity of the complexes. R. M. has performed the electrochemical experiments. C. N. helped plan the experiments. S. C. and J. A. write the manuscript and plan the experiments.

Acknowledgments

We acknowledge grants financed by the Spanish Government (SAF2012-34424, CTQ-2012-37420-C02-02). P.S. thanks the Erasmus Programme for a research stipend, and L.M. and T.M. acknowledge AIRC (IG12085) and Beneficentia Stiftung (Vaduz) for generous financial support. We also thank the members of COST Action CM1105 for useful discussions. J.A. thanks the Spanish MICINN for his "Ramón y Cajal" contract.

Appendix A. Supplementary data

Supplementary data to this article can be found online at http://dx.doi.org/10.1016/j.jinorgbio.2015.09.012.

References

[1] P. Ivo da Silva, V.M.D.D. Maia, U. Abram, Future Med. Chem. 6 (2014) 1515.
[2] B. Bertrand, A. Casini, Dalton Trans. 43 (2014) 4209.
[3] N. Cutillas, G.S. Yellol, C. de Haro, C. Vicente, V. Rodríguez, J. Ruiz, Coord. Chem. Rev. 257 (2013) 2784.
[4] F. Cisnetti, A. Gautier, Angew. Chem. Int. Ed. 52 (2013) 11976.
[5] S.J. Berners-Price, A. Filipovska, Metallomics 3 (2011) 863.
[6] C.-M. Che, R.W.-Y. Sun, Chem. Commun. 47 (2011) 9554.
[7] I. Ott, Coord. Chem. Rev. 253 (2009) 1670.
[8] X. Wang, Z. Guo, Dalton Trans. (2008) 1521.
[9] T. Zou, C.T. Lum, S.S.-Y. Chui, C.M. Che, Angew. Chem. Int. Ed. 52 (2013) 2930.
[10] S.D. Köster, H. Alborzinia, S. Can, I. Kitanovic, S. Wölfl, R. Rubbiani, I. Ott, P. Riesterer, A. Prokop, K. Merz, N. Metzler-Nolte, Chem. Sci. 3 (2012) 2062.
[11] A. Casini, C. Hartinger, C. Gabbiani, E. Mini, P.J. Dyson, B.K. Keppler, L. Messori, J. Inorg. Biochem. 102 (2008) 562.
[12] L. Ronconi, L. Giovagnini, C. Marzano, R. Bettio, R. Graziani, G. Pilloni, D. Fregona, Inorg. Chem. 44 (2005) 1867.
[13] A. Casini, L. Messori, Curr. Top. Med. Chem. 11 (2011) 2647.
[14] G. Marcon, L. Messori, P. Orioli, Expert. Rev. Anticancer. Ther. 2 (2002) 338.
[15] G. Marcon, S. Carotti, M. Coronello, L. Messori, E. Mini, P. Orioli, T. Mazzei, M.A. Cinellu, G. Minghetti, J. Med. Chem. 45 (2002) 1672.
[16] L. Messori, F. Abbate, G. Marcon, P. Orioli, M. Fontani, E. Mini, T. Mazzei, S. Carotti, T. O'Connell, P. Zanello, J. Med. Chem. 43 (2000) 3541.
[17] N.G. Faux, C.W. Ritchie, A. Gunn, A. Rembach, A. Tsatsanis, J. Bedo, J. Harrison, L. Lannfelt, K. Blennow, H. Zetterberg, M. Ingelsson, C.L. Masters, R.E. Tanzi, J.L. Cummings, C.M. Herd, A.I. Bush, J. Alzheimers Dis. 20 (2010) 509.
[18] S.K. Prashant, A.K. Dutta, Curr. Bioact. Compd. 4 (2008) 57.
[19] A.I. Bush, R.E. Tanzi, Neurotherapeutics 5 (2008) 421.
[20] K.J. Barnham, E. Gautier, L. Colette, G.B. Kong, G. Krippner, 8-hydroxy quinoline derivatives, WO 2004/007461, 2004.
[21] H.R. Dholariya, K.S. Patel, J.C. Patel, A.K. Patel, K.D. Patel, Med. Chem. Res. 22 (2013) 5848.
[22] B. Choi, J. Young, G. Bong, J.H. Kim, J.-N. Seo, G. Wu, M. Sohn, T.N. Chung, S.W. Suh, Neurobiol. Dis. 54 (2013) 382.
[23] A.D. Schimmer, Y. Jitkova, M. Gronda, Z. Wang, J. Brandwein, C. Chen, V. Gupta, A. Schuh, K. Yee, J. Chen, S. Ackloo, T. Booth, S. Keays, M.D. Minden, Clin. Lymphoma Myeloma Leuk. 12 (2012) 330.
[24] C.M. Darby, C.F. Nathan, J. Antimicrob. Chemother. 65 (2010) 1424.
[25] H. Jiang, J.E. Taggart, X. Zhang, D.M. Benbrook, S.E. Lind, W.-Q. Ding, Cancer Lett. 312 (2011) 11.
[26] K.G. Daniel, D. Chen, S. Orlu, Q.C. Cui, F.R. Miller, Q.P. Dou, Breast Cancer Res. 7 (2005) R897.
[27] X. Mao, X. Li, R. Sprangers, X. Wang, A. Venugopal, T. Wood, Y. Zhang, D.A. Kuntz, E. Coe, S. Trudel, D. Rose, R.A. Batey, L.E. Kay, A.D. Schimmer, Leukemia 23 (2009) 585.
[28] D. Chen, Q.C. Cui, H. Yang, R.A. Barrea, F.H. Sarkar, S. Sheng, B. Yan, G.P. Reddy, Q.P. Dou, Cancer Res. 67 (2007) 1636.
[29] S.M. Zhai, L. Yang, Q.C. Cui, Y. Sun, Q.P. Dou, B. Yan, J. Biol. Inorg. Chem. 15 (2010) 259.
[30] H. Yu, Y. Zhou, S.E. Lind, W.Q. Ding, Biochem. J. 417 (2009) 133.
[31] W.Q. Ding, B. Liu, J.L. Vaught, H. Yamauchi, S.E. Lind, Cancer Res. 65 (2005) 3389.
[32] H. Yu, J.R. Lou, W.Q. Ding, Anticancer Res. 30 (2010) 2087.
[33] T. Du, G. Filiz, A. Caragounis, P.J. Crouch, A.R. White, J. Pharmacol. Exp. Ther. 324 (2008) 360.
[34] J. Alemán, V. Solar, A. Álvarez-Valdés, J.M. Padrón, C. Ríos-Lucí, C. Navarro-Ranninger, MedChemCommun 2 (2011) 789.
[35] V. del Solar, A. Quinones-Lombrana, S. Cabrera, J.M. Padrón, C. Rios-Luci, A. Alvarez-Valdes, C. Navarro-Ranninger, J. Alemán, J. Inorg. Biochem. 127 (2013) 128.
[36] C. Pérez, V. Díaz-García, A. Agudo-López, V. del Solar, S. Cabrera, M. Teresa Agulló-Ortuño, C. Navarro-Ranninger, J. Alemán, J.A. López-Martín, Eur. J. Med. Chem. 76 (2014) 360.
[37] C. Martín Santos, S. Cabrera, C. Ríos-Luci, J.M. Padrón, I. López Solera, A.G. Quiroga, M.A. Medrano, M.C. Navarro-Ranninger, J. Alemán, Dalton Trans. 42 (2013) 13343.
[38] SAINT+v7.12a. Area-Detector Integration Program, Bruker-Nonius AXS, Madison, Wisconsin, USA, 2004.
[39] G.M. Sheldrick, SADABS Version 2004/1, A Program for Empirical Absorption Correction, University of Göttingen, Göttingen, Germany, 2004.
[40] SHELXTL-NT version 6.12, Structure Determination Package, Bruker-Nonius AXS, Madison, Wisconsin, USA, 2001.
[41] K. Bracht, Boubakari, R. Grünert, P.J. Bednarski, Anti-Cancer Drugs 17 (2006) 41.
[42] A.G. Quiroga, J.M. Pérez, I. López-Solera, E.I. Montero, J.R. Masaguer, C. Alonso, C. Navarro-Ranninger, J. Inorg. Biochem. 69 (1998) 275.
[43] S. Tardito, A. Barilli, I. Bassanetti, M. Tegoni, O. Bussolati, R. Franchi-Gazzola, C. Mucchino, L. Marchiò, J. Med. Chem. 55 (2012) 10448.
[44] M. Patra, T. Joshi, V. Pierroz, K. Ingram, M. Kaiser, S. Ferrari, B. Spingler, J. Keiser, G. Gasser, Chem. Eur. J. 19 (2013) 14768.
[45] M.D. Hall, K.A. Telma, K.-E. Chang, T.D. Lee, J.P. Madigan, J.R. Lloyd, I.S. Goldlust, J.D. Hoeschele, M.M. Gottesman, Cancer Res. (2014) 3913.
[46] A. Casini, A. Guerri, C. Gabbiani, L. Messori, J. Inorg. Biochem. 102 (2008) 995.